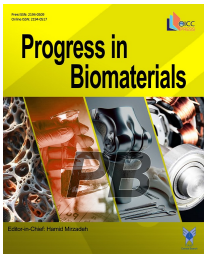

Volume 13, Issue 3, 132412 (1-8)

Progress in Biomaterials (PIBM)

https://doi.org/10.57647/pibm.2024.132412

Modulation of Optical Anisotropy in Soft Tissue Biomaterials Using Optical Clearing Agents: Implications for Structural Characterization and Biomedical Applications

Saeed Ziaee[1], Mohammad Ali Ansari[1,*], Mehrdad Kalhori[1], Kamyab Hassani[1], Mohammad Hossein Naddaf[1], Valery V. Tuchin[2,3,4]

[1]*Laser and Plasma Research Institute, Shahid Beheshti University, Tehran 19839 69411, Iran.*
[2]*Institute of Physics and Science Medical Center, Saratov State University, 83 Astrakhanskaya str., Saratov 410012, Russia.*
[3]*Laboratory of Biophotonics, Tomsk State University, TTomsk 634050, Russia.*
[4]*Institute of Precision Mechanics and Control, FRC "Saratov Scientific Centre of the RAS", Saratov 410028, Russia.*

[*]**Corresponding author:** m_ansari@sbu.ac.ir

Original Research

Abstract:

This study systematically investigates the modulation of optical properties in anisotropic chicken skin tissue using five optical clearing agents (OCAs): Sorbitol, Glycerol, Iohexol, Sucrose, and Glucose. Quantifying such changes is essential for the design of biomaterials and the optimization of tissue-implant interfaces where laser propagation is critical. Utilizing goniometry and transmission spectroscopy over a 60-minute period, our results consistently demonstrated that tissue optical clearing induced a significant increase in the scattering anisotropy factor (g), shifting from a baseline of $g = 0.78 - 0.80$ to post-clearing values reaching $g = 0.96$. This enhancement in forward scattering, accompanied by a concurrent decrease in the attenuation coefficient (μ_t), serves as a critical performance metric for improving the Signal-to-Noise Ratio (SNR) in implanted optical sensors and ensuring efficient laser light delivery in photo-active scaffolds. Among the agents, Sorbitol exhibited the highest optical clearing efficacy, while simple sugars showed less pronounced effects. These findings provide a robust foundation for selecting optimal chemical agents to enhance laser light penetration depth for future embedded optical biosensors, directly benefiting the development of advanced biomaterials, and high-resolution imaging modalities such as Optical Coherence Tomography (OCT).

Keywords:

Tissue optical clearing; Scattering anisotropy factor; Structural characterization; Biological tissue Green laser

Cite this article: Ziaee, S., Ansari, M.A., Kalhori, M., Hassani, K., Naddaf, M.H., Tuchin, V.V. Modulation of Optical Anisotropy in Soft Tissue Biomaterials Using Optical Clearing Agents: Implications for Structural Characterization and Biomedical Applications. *Progress in Biomaterials* **13**(3), Article 12 (2024).

1. Introduction

Optical characterization of soft biological tissues, such as skin and muscle, is a critical prerequisite for enhancing both diagnostic imaging and therapeutic techniques. Light-tissue interactions are fundamentally governed by a set of key optical parameters, including the anisotropy coefficient or factor (g), the absorption coefficient (μ_a), the scattering coefficient (μ_s), and the attenuation coefficient ($\mu_t = \mu_a + \mu_s$) (Shanshool et al., 2024; Cheong et al., 1990; Jacques, 2013, 1996). A comprehensive understanding of the origins and behavior of these optical properties is necessary across the ultraviolet (UVA), visible, and near-infrared (NIR) regions for developing accurate tissue models. Understanding these parameters in easily accessible tissues, such as those from mice and chickens, commonly used in biomedical research, is essential for successful translational applications. The anisotropy coefficient plays a defining role as it quantifies the directionality of photon scattering within the biomaterial tissues (Marquez et al., 1998; Wang et al., 1995).

Tissue anisotropy arises directly from the underlying structural organization, most notably the alignment of muscle fibers, which leads to pronounced direction-dependent light

scattering. Studies have conclusively demonstrated that the orientation of muscle fibers significantly affects measured optical properties, with variations in probe orientation relative to muscle fibers in chicken breast tissue resulting in differing absorption and reduced-scattering coefficients. This highly anisotropic behavior necessitates its precise characterization to ensure accurate modeling of light propagation in tissues, often involving complex computational methods such as Monte Carlo modeling of light transport in multi-layered tissues. The determination of g and other critical parameters, such as the transmission spectrum (T_c) and attenuation, is achieved through specialized techniques, including goniometry and transmission spectroscopy. Furthermore, research into the optical properties of human tissues, including brain and skin, highlights the broad relevance of these fundamental parameters (Zhu et al., 2013; Hirshburg et al., 2007; Genina et al., 2005). To mitigate the limitations imposed by light scattering and to enhance optical imaging depth and clarity, optical clearing techniques have been extensively developed. These methods aim to reduce light scattering within tissues by employing chemical agents, such as glycerol and polyethylene glycol, to alter the refractive index of tissue components, thereby minimizing scattering mismatches. This agent-based approach has been shown to significantly decrease the attenuation coefficient, facilitating deeper light penetration (Genin et al., 2016; Bashkatov et al., 2011; Tuchina et al., 2016). Recent studies have explored the efficacy of various compounds, including sugars and sugar alcohols like sorbitol, as potent optical clearing agents, interacting with collagen in the skin to reduce light scattering. For instance, dextrose, fructose, sucrose, and sorbitol have demonstrated superior collagen solubility and optical clearing potential compared to glycerol in rodent skin. Molecular dynamics simulations further support this, revealing that sugars forming more hydrogen bonds with collagen peptides exhibit higher optical clearing efficacy. The successful application of these agents in diverse tissues, including human dura mater, has been achieved. Given that modifications in tissue composition or structure influence the attenuation coefficient, and considering the central role of g-factor in scattering, understanding the effect of these clearing solutions on the anisotropy coefficient is essential for interpreting optical imaging results and for developing accurate tissue models (Marquez et al., 1998; Samatham et al., 2010; Shariati et al., 2023; Shariati et al., 2022; Tuchina et al., 2019; Hirshburg et al., 2010; Yaroslavsky et al., 2002). This knowledge is also key for the application of advanced imaging techniques like Dynamic Optical Coherence Tomography (OCT) in the study of optical clearing effects. From a biological perspective, the optical behavior of skin is intrinsically linked to its complex hierarchical organization, where the dermis acts as a highly scattering medium primarily due to the dense, semi-ordered network of collagen fibers. The scattering anisotropy factor is a direct reflection of this structural alignment; thus, quantifying its dynamic changes during optical clearing provides a unique window into the reorganization and refractive index matching of these biological constituents. Regarding biomedical applications, the ability to systematically increase the g-factor toward forward scattering (reaching up to $g = 0.96$ as shown in this study) is fundamental for overcoming the "scattering barrier" in deep-tissue imaging. These findings are highly motivated by the need for enhanced precision in photodynamic therapy (PDT) and laser surgery, where accurate dosimetry depends on precise light distribution models. Furthermore, the derived parameters for agents like sorbitol and glycerol offer critical input for optimizing high-resolution diagnostic tools such as OCT and fluorescence microscopy, ultimately facilitating clearer visualization of pathological changes in anisotropic biomaterial tissues. Ultimately, investigating the optical properties of tissues, with a distinct focus on the anisotropy coefficient, provides a pathway for the optimization of optical imaging techniques and enhances our fundamental understanding of light-tissue interactions in anisotropic biological media (Larin and Tuchin, 2008; Zonios and Dimou, 2009; Tuchin et al., 2002).

This study aims to systematically investigate the optical properties (g, μ_t, μ_s, and T_c) of chicken skin, focusing on the anisotropy coefficient at 532 nm wavelength. By applying various optical clearing solutions, we seek to elucidate their effects on biomaterial tissue transparency and light propagation. The findings are expected to contribute to the optimization of optical imaging techniques and enhance our understanding of light-tissue interactions in anisotropic biomaterial tissues.

2. Materials and methods

Fifteen chicken skin samples were prepared ($\sim 1.5 \times 1.5$ cm^2, and $0.54 \sim 0.88$ mm thickness). Five different clearing agents were subsequently applied to the skins, including glycerol, sorbitol, 40% glucose, 60% sucrose, iohexol. The prepared samples were placed inside a rectangular glass chamber. Goniometric experiments were then performed to determine the anisotropy parameter at eleven distinct time points: before clearing, and 6 to 60 minutes after clearing. Furthermore, transmission (T_c) acquired, and the attenuation coefficient (μ_t) was calculated from these spectral data. The goniometric setup (illustrated in figure 1) comprised a green diode laser (532 nm wavelength with a maximum output power of 100 mW, Mahfanavar, Iran), a circular plate for sample mounting, a chamber holding the sample and the OCA, and a biased detector (DET10A, Thorlabs, active area 0.8 mm^2 (⌀1.0 mm), Field of view is 1.45 cm, wavelength $200-1100$ nm, raise time 1 ns, bandwidth 350 MHz, bias voltage 10 V, dimension 48.0 mm $\times$ 21.1 mm $\times$ 70.1 mm) mounted on a stepper motor (Leadshine Nema 23 Stepper Motor (2.3 N·m, 5.0 A) with a 1.8º step angle, rated volt 1.9 V, motor length 76 mm, China) that rotated the sample in increments of 5 degrees (36 steps from 0° to $+90°$ and $-90°$ degrees). The scattered intensity from the sample was recorded using a recording device (PDA200C photodiode amplifier, Thorlabs, six current ranges from 100 nA to 10 mA full scale and provides a maximum display resolution of 10 pA, bias voltage 0 to -10 V (CG) and 0 to $+10$ V (AG)m noise $\leq 0.02\%$). This photodiode amplifier connected to DET10A photodetector using a BNC cable.

For the acquisition of the transmission spectra and the sub-

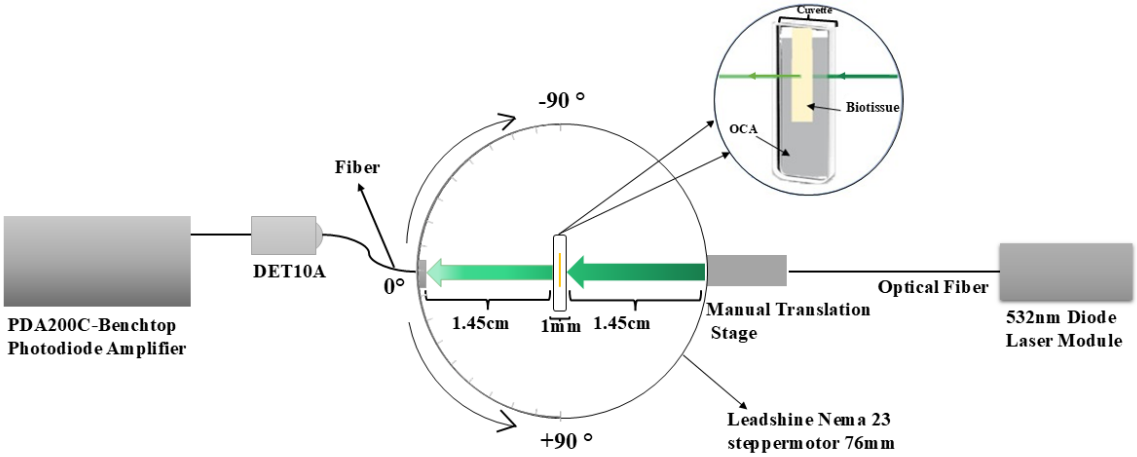

Figure 1. This meticulously assembled system features a 532 nm green diode laser for precise illumination of the sample, which is housed within a custom chamber containing the OCA. The setup employs a biased photodetector (DET10A) mounted on a stepper motor (1.8° step angle) to record the scattered light intensity with 5-degree angular resolution. Data integrity is maintained by the high-sensitivity Photodiode Amplifier (PDA200C), ensuring robust and accurate measurement of optical scattering parameters.

sequent calculation of the attenuation coefficient from the transmission spectrum, same devices used as in goniometry setup, as shown in figure 1.

To calculate the anisotropy factor (g) of biological tissue, as investigated by Wilson and Adam (1983), Jacques et al. (1988), and Parsa et al. (1989), the photons are predominantly scattered in the forward direction. This pronounced forward scattering phenomenon cannot be adequately explained by Rayleigh scattering. Furthermore, the wavelength dependence of the scattering observed in biological tissue is typically slightly stronger than that predicted by Mie scattering theory. Consequently, neither Rayleigh nor Mie scattering models are fully capable of describing the complex scattering behavior within tissues. Therefore, it is essential to define a probability distribution function $p(\theta)$ for a photon scattered at a specific angle θ that can be accurately fitted to the experimental goniometric data. It is explicit that the value of the scattering anisotropy factor (g) must be constrained within the range $0 \leq g \leq 1$ for biological tissue, as $p(\theta)$ depends on θ. In the general theory of light scattering, the interpretation of this coefficient is as follows: $g = 1$ signifies complete forward scattering (the photon's direction is unchanged). $g = 0$ represents isotropic scattering (scattering is equally likely in all directions). Also, $g = -1$ indicates complete backward scattering (the photon is reflected directly backward, 180°). Thus, if anisotropy is defined in polar coordinates (Jacques, 2013; Bashkatov et al., 2011; Wilson and Adam, 1983; Jacques et al., 1988; Parsa et al., 1989; Oliveira and Tuchin, 2019; Niemz, 2014; Tuchin, 2015):

$$g = \frac{\int_{4\pi} p(\theta)\cos(\theta)d\omega}{\int_{4\pi} p(\theta)d\omega}, \tag{1}$$

where $p(\theta)$ is a probability function and $d\omega = \sin\theta d\theta d\phi$ is the elementary solid angle.

Therefore, the anisotropy factor (g) is a fundamental parameter that characterizes the angular distribution of single-scattering events (it only depends on the angle between the photon directions before and after the scattering event) and is formally defined as the average cosine of the scattering angle (θ):

$$g = \langle \cos\theta \rangle \tag{2}$$

For most biological tissues, it can be stated that the anisotropy factor (g) typically falls within the range from 0.70 to 0.99.

Since the probability function, also known as the phase function $p(\theta)$, is inherently normalized,

$$\frac{1}{4\pi}\int_{4\pi} p(\theta)d\omega = 1 \tag{3}$$

The ideal fit to experimental observations can be determined by considering several existing theoretical phase functions. These functions typically include the Henyey-Greenstein (HG) function, the Rayleigh-Gans function, and the δ-Eddington approximation. The most effective model is frequently found to be the HG phase function. Consequently, the probability distribution function $p(\theta)$ for a single scattering event can be expressed as:

$$p(\theta) = \frac{1}{4\pi}\frac{1-g^2}{(1+g^2-2g\cos\theta)^{3/2}} \tag{4}$$

This phase function is mathematically very convenient to handle since it is equivalent to the representation:

$$p(\theta) = \sum_{i=0}^{\infty}(2i+1)g^i P_i(\cos\theta) \tag{5}$$

Consequently, the anisotropy coefficient, g, can be independently derived from angular measurements of scattered light intensity (I). This is achieved using a goniometric setup to record the intensity across various scattering angles (θ). Mathematically, the scattering anisotropy coefficient, g, is defined as the average cosine of the scattering angle, θ, as expressed in Eq. (1)-(6) (Sardar et al., 2001; Fernández-Oliveras et al., 2012).

$$g = \frac{\sum_i(\cos\theta_i)I_i}{\sum_i I_i}, \quad i = 0, 1, \ldots, 12 \tag{6}$$

Finally, the essential relationship between the scattering coefficient, or μ_s, (a measure of the number of photons that are scattered in the medium per unit length of the beam path) and the anisotropy factor (g) is conventionally expressed by defining the reduced scattering coefficient ($\acute{\mu}_s$) as follows (Oliveira and Tuchin, 2019):

$$\acute{\mu}_s = \mu_s(1-g) \tag{7}$$

In this manner, the anisotropy factor (g) becomes a crucial tool for studying diffuse media, such as soft biomaterial tissues and their related optical parameters. Specifically, g enables the quantitative investigation of scattering anisotropy media. For the purposes of this study, this methodology is essential for characterizing the effect of the OCAs on the tissue scattering anisotropy properties.

In addition, after obtaining the transmission spectrum, the following equation is used to obtain the attenuation coefficient (Oliveira and Tuchin, 2019; Tuchin et al., 2021):

$$T_c = e^{-\mu_t d}, \tag{8}$$

where d is thickness of the sample slab.

In general, the attenuation coefficient of a medium is fundamentally defined as the sum of the scattering coefficient and the absorption coefficient ($\mu_t = \mu_s + \mu_a$) caused by that medium. So, for highly turbid media, such as biological tissues, the μ_s significantly dominates the μ_a.

Consequently, the μ_t can be accurately approximated by the μ_s (Shanshool et al., 2024; Oliveira and Tuchin, 2019; Tuchin et al., 2021):

$$\text{If } \mu_s \gg \mu_a, \text{ then } \mu_t \approx \mu_s.$$

Consequently, determining the attenuation coefficient allows for the derivation of an approximation of the dispersion coefficient.

3. Results

As anticipated from the figure 2, the results indicate that the anisotropy coefficient increased following the application of the OCA(s) from 0° to +90° and −90° degrees. This signifies an enhancement in forward scattering, leading to the light being more strongly forward directed. Therefore, it can be concluded that the anisotropy coefficient is not only wavelength-dependent (such as studies like (Bashkatov et al., 2011; Fukutomi et al., 2016), from 325 nm to 1557 nm) but also increases at a random wavelength, 532 nm, contingent upon the type of OCAs employed.

By obtaining the thickness of the samples and the transmittance spectrum and subsequently inputting these into Eq. (1)-(8), the changes in the attenuation coefficient are reported in Table 1. This table further substantiates that tissue optical clearing is accompanied by both an increase in the transmittance spectrum and a concurrent decrease in the attenuation coefficient. This result is in complete agreement with the conclusion drawn from Fig. 2.

According to figure 2 and Table 1, it can be seen that sorbitol induces the greatest changes in tissue anisotropy and μ_t reduction, followed by glycerol and iohexol, which exhibit similar behavior. sugars also increase anisotropy, but their effect is less pronounced than that of the other agents. These findings offer a better understanding of tissue clearing and the associated increase in light penetration depth. Therefore, examining the changes in the anisotropy coefficient is highly beneficial for two primary reasons: First, in understanding the mechanisms of light interaction with tissue during optical clearing, and second, in significantly aiding the enhancement of light penetration depth in the tissue. Also, as time increases, it can be seen from Fig. 3. that the kinetics of OCAs penetration into the tissue is increasing, so it can be concluded a direct relationship with the increase in the g-factor.

4. Discussion

The fundamental goal of this study was to systematically investigate the effect of various OCAs on the anisotropy coefficient and μ_t of anisotropic chicken skin tissue, providing crucial insights into the mechanisms of light-tissue interaction. The core finding that tissue clearing is accompa-

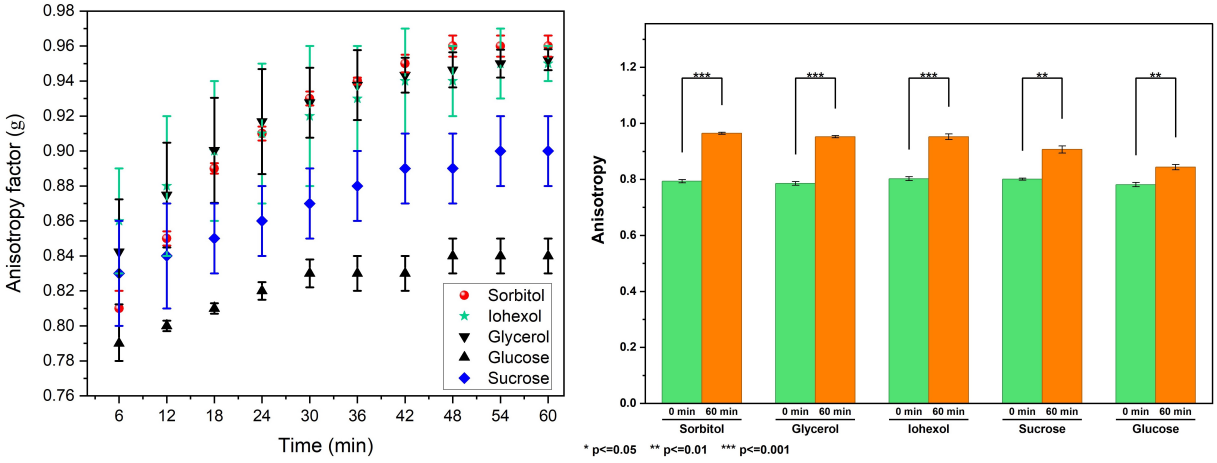

Figure 2. Changes in tissue anisotropy following treatment with five different OCAs, sorbitol, glycerol, iohexol, sucrose, and glucose. Data are presented as the mean ± standard deviation for each group, with N = 3 replicates per OCAs, * p <= 0.05, ** p <= 0.01, *** p <= 0.001. Left, the graph shows the changes in the anisotropy coefficient over a 60-minute clearing period. Right, the data indicate a significant difference between the baseline (before clearing) and the 60-minute time point (after clearing).

Table 1. Measured transmission spectrum, sample thickness, and calculated μ_t of chicken skin tissue, before and after 60 min clearing, treated with five different OCAs, sorbitol, glycerol, iohexol, sucrose, and glucose.

Agent	Time	Thickness (mm)	T_C	μ_t (mm^{-1})	g
Sorbitol	Before	0.54	0.011	8.35 ± 0.45	0.79 ± 0.01
	After	0.41	0.266	3.22 ± 0.22	0.96 ± 0.02
Glycerol	Before	0.88	0.010	5.23 ± 0.18	0.78 ± 0.01
	After	0.57	0.222	2.64 ± 0.3	0.95 ± 0.01
Iohexol	Before	0.59	0.015	7.11 ± 0.4	0.80 ± 0.02
	After	0.53	0.231	2.76 ± 0.16	0.95 ± 0.01
Sucrose	Before	0.62	0.018	6.47 ± 0.12	0.80 ± 0.01
	After	0.43	0.110	5.13 ± 0.5	0.90 ± 0.02
Glucose	Before	0.77	0.007	6.44 ± 0.28	0.78 ± 0.02
	After	0.60	0.022	6.36 ± 0.31	0.84 ± 0.03

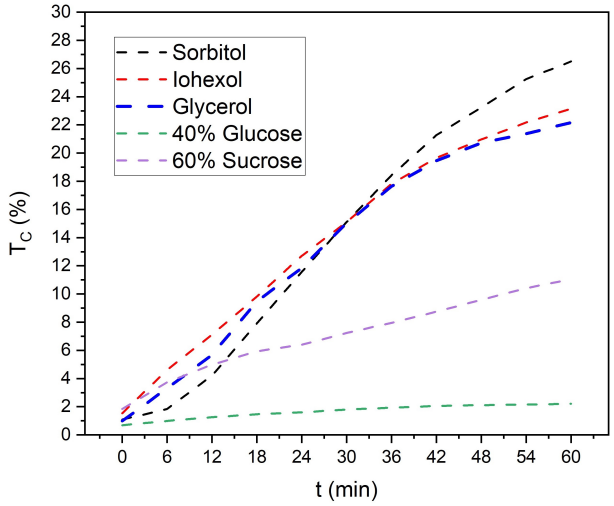

Figure 3. Kinetics of OCAs over time during skin clearing.

nied by a significant increase in the anisotropy coefficient is consistent across all tested agents. This shift toward higher g-factor values—ranging from a pre-clearing baseline of $g = 0.78 - 0.80$ to post-clearing values as high as $g = 0.96$ quantifies an essential enhancement in forward scattering. Physically, this indicates a substantial reduction in the angular randomization of photons, leading to light being more strongly directed forward and consequently, deeper penetration within the tissue.

The increases in the anisotropy factor (g-factor) are directly linked to the underlying structural changes induced by the OCAs. Given that g-factor quantifies the directionality of scattering, its increase suggests that the refractive index mismatch between the scattering structures (primarily collagen fibers in the dermal layer of skin) and the surrounding ground substance is being minimized and the collagen fibers are being rendered more ordered due to tissue shrinkage caused by its dehydration (Tuchin, 2015; Tuchin et al., 2021). Beyond diagnostic applications, the ability of OCAs to modulate tissue anisotropy provides fundamental insights into the structural dynamics of the extracellular matrix (ECM). Our results demonstrate that the shift in the g-factor reflects the reorganization of collagen fibers and the reduction of refractive index mismatches. This understanding is pivotal for the design and optimization of biomaterials and scaffolds, where mimicking the natural anisotropic scattering of host tissues is essential for seamless integration. Furthermore, quantifying light-tissue interactions at tissue interfaces is critical for the development of smart implants and wearable optical sensors. By precisely characterizing how chemical agents alter the transparency and directionality of light in anisotropic media, researchers can better predict the performance of optical interfaces in contact with biological environments, ensuring more efficient energy delivery and signal acquisition in bio-implanted devices. Specifically, the presented results can be mapped onto critical biomaterial performance metrics. The significant increase in the g-factor from 0.80 to 0.96 directly translates to an improvement in the SNR for optical biosensors embedded within or beneath the tissue. High anisotropy ensures that more ballistic photons reach the detector, minimizing the background noise caused by multiple scattering events. Furthermore, the reduction in the attenuation coefficient (μ_t) achieved by agents like Sorbitol serves as a metric for light delivery efficiency; this is vital for the performance of photo-active scaffolds used in tissue engineering, where deep and uniform light distribution is required for cell activation or polymerization. So, the ob-

served stability of these optical parameters over 60 minutes provides a benchmark for the operational longevity of temporary optical clearing-based interfaces, ensuring that the material performance remains predictable during the critical window of a surgical or diagnostic procedure.

The application of OCAs, such as glycerol and sugar solutions, is known to displace water, infiltrate the tissue matrix, and thereby match the refractive indices of collagen (or other structural components) and the extracellular fluid (Tuchin, 2015; Tuchin et al., 2021; Wang et al., 2014; Sudheendran et al., 2010; Moulton et al., 2006). This reduction in the refractive index difference significantly lowers the overall scattering coefficient, which, according to the reduced scattering coefficient definition, must be accompanied by an increase in g-factor to maintain consistency or to achieve the observed reduction in overall attenuation (Shanshool et al., 2024; Wang et al., 2014; Sudheendran et al., 2010; Moulton et al., 2006).

The observed time-dependent increase in g-factor over the 60-minute tissue clearing period further validates the kinetics of OCA diffusion into the tissue matrix (as shown OCAs kinetics in Fig. 3). Among the five tested agents, Sorbitol induced the greatest changes, resulting in the highest g-factor value and the most significant reduction. Glycerol and iohexol followed, exhibiting similar behavior in both anisotropy enhancement and attenuation reduction, which is consistent with their known efficacy as potent OCAs. Conversely, the simpler sugars (Sucrose and Glucose) also increased anisotropy, but their effect was demonstrably less pronounced. This differential efficacy aligns with previous research in Ziaee et al. (2023) suggesting that molecular properties-such as the number of hydrogens bonds a sugar form with collagen peptides and its solubility-play a critical role in its clearing potential. The superior performance of Sorbitol (a sugar alcohol) likely stems from its optimized molecular structure and interaction capabilities with the collagen matrix of the chicken skin, leading to a more effective index matching compared to the tested sugar solutions.

A notable finding of this study is the confirmation that the observed increase in g-factor occurred at a random wavelength (532 nm). This adds to the existing body of literature which had previously demonstrated that the anisotropy coefficient is not only wavelength-dependent, but that its modification by OCAs can be specific to certain spectral ranges. This result is in strong agreement with prior results (but in 488 nm) by Samatham et al. (2010) had shown this specific change experimentally, although only for glycerol, while Tuchin et al. (2021) had shown similar behavior in computational simulations. Our study extends these findings by experimentally validating this wavelength-specific anisotropy increase for a panel of five different OCAs, demonstrating that this behavior is a generalized response of strongly scattering tissue to a variety of clearing agents, rather than an isolated phenomenon unique to glycerol.

The simultaneous increase in g-factor and decrease in μ_t (as substantiated by the collimated transmittance) highlights the combined benefit of tissue optical clearing. A higher g-factor value means less photon randomization (more forward-directed light), and a lower μ_t means fewer overall losses, both synergistically contributing to a significantly enhanced light penetration depth. This detailed characterization of the anisotropy coefficient is therefore highly beneficial for two primary reasons: First, it refines our mechanistic understanding of how different OCA interact with and reorganize tissue structure to reduce scattering; and second, it provides essential parameters for improving the accuracy of computational models, such as Monte Carlo simulations, which are critical for planning photodynamic therapy or optimizing advanced imaging techniques like Dynamic OCT. The data presented here establish a robust foundation for selecting the optimal OCA based on desired optical performance in soft biomaterial tissues.

5. Conclusion

To investigate the scattering anisotropy coefficient of chicken skin tissue, five optical clearing agents OCAs-sorbitol, glycerol, iohexol, sucrose, and glucose-were employed. Measurements were conducted at a wavelength of 532 nm over a 60-minute period, with data collected at 6-minute intervals. The results demonstrated that an increase in g-factor was accompanied by a concurrent decrease in the attenuation coefficient. Among the agents tested, sorbitol exhibited the highest clearing efficacy, while glucose showed the lowest optical clearing potential.

The detailed characterization of the g-factor and its dynamic changes is highly beneficial for both scientific and clinical advancement. As established, tissue anisotropy arises notably from the alignment of fibers, like muscle fibers, which governs light scattering direction. The precise, time-resolved g and μ_t values derived are essential input parameters for improving the accuracy of computational light models, such as Monte Carlo simulations, which are critical for predicting light distribution during treatments. This quantitative data also enables more accurate dosimetry planning for laser-based therapies like Photodynamic Therapy (PDT), and directly benefits high-resolution imaging modalities such as Dynamic OCT by providing a pathway to enhance penetration depth and clarity. Finally, this study provides fundamental, quantitative insights into the modification of tissue optical properties by a diverse panel of OCAs, establishing a robust foundation for the rational design and optimization of future optical biosensors embedded within or beneath the brain tissues for diagnostic and therapeutic applications.

Acknowledgement

This work is based upon research funded by Iran National Science Foundation (INSF) under project number 98029460.

VVT was supported by the Russian Science Foundation grant, No. 24-44-00082.

Authors contributions
All authors contributed equally to the conception, design, execution, and writing of this work. All authors read and approved the final manuscript.

Availability of data and materials
The datasets generated during and/or analyzed during the current study are available from the corresponding author on reasonable request.

Conflict of interests
The authors declare that they have no known competing financial interests or personal relationships that could have appeared to influence the work reported in this paper.

References

Bashkatov A. N., Genina E. A., Tuchin V. V. (2011) Optical properties of skin, subcutaneous, and muscle tissues: A review. *J. Innov. Opt. Health Sci.* 4 (1): 9–38. DOI: https://doi.org/10.1142/S1793545811001319.

Cheong W. F., Prahl S. A., Welch A. J. (1990) A Review of the Optical Properties of Biological Tissues. *IEEE J. Quantum Electron* 26 (12): 2166–2185. DOI: https://doi.org/10.1109/3.64354.

Fernández-Oliveras A., Rubiño M., Perez M. M. (2012) Scattering anisotropy measurements in dental tissues and biomaterials. *J. Eur. Opt. Soc. Publ.* 7:12016. DOI: https://doi.org/10.2971/jeos.2012.12016.

Fukutomi D., Ishii K., Awazu K. (2016) Determination of the scattering coefficient of biological tissue considering the wavelength and absorption dependence of the anisotropy factor. *Opt. Rev.* 23 (2): 291–298. DOI: https://doi.org/10.1007/s10043-015-0161-y.

Genin V., Tuchina D., Sadeq A. J., Genina E., Tuchin V., Bashkatov A. (2016) *Ex vivo* investigation of glycerol diffusion in skin tissue. *J. Biomed. Photonics Eng.* 2 (1): 010303–1–010303–5. DOI: https://doi.org/10.18287/jbpe16.02.010303.

Genina E. A., Bashkatov A. N., Kochubey V. I., Tuchin V. V. (2005) Optical clearing of human dura mater. *Opt. Spectrosc. (English Transl. Opt. i Spektrosk.)* 98 (3): 470–476. DOI: https://doi.org/10.1134/1.1890530.

Hirshburg J., Choi B., Nelson J. S., Yeh A. T. (2007) Correlation between collagen solubility and skin optical clearing using sugars. *Lasers Surg. Med.* 39 (2): 140–144. DOI: https://doi.org/10.1002/lsm.20417.

Hirshburg J. M., Ravikumar K. M., Hwang W., Yeh A. T. (2010) Molecular basis for optical clearing of collagenous tissues. *J. Biomed. Opt.* 15 (5): 055002. DOI: https://doi.org/10.1117/1.3484748.

Jacques S. L. (2013) Corrigendum: Optical properties of biological tissues: a review. *Phys. Med. Biol.* 58 (14): 5007–5008. DOI: https://doi.org/10.1088/0031-9155/58/14/5007.

——— (1996) Origins of Tissue Optical Properties in the UVA, Visible, and NIR Regions. *Advances in Optical Imaging and Photon Migration* Washington, D.C.: Optica Publishing Group:OPC364. DOI: https://doi.org/10.1364/AOIPM.1996.OPC364.

Jacques S. L., Alter C. A., Prahl S. A. (1988) Angular dependence of HeNe laser light scattering by human dermis. *Lasers Life Sci.* 2 (4): 309–333.

Larin K. V, Tuchin V. V (2008) Functional imaging and assessment of the glucose diffusion rate in epithelial tissues in optical coherence tomography. *Quantum Electron.* 38 (6): 551–556. DOI: https://doi.org/10.1070/qe2008v038n06abeh013850.

Marquez G., Wang L. V., Lin S.-P., Schwartz J. A., Thomsen S. L. (1998) Anisotropy in the absorption and scattering spectra of chicken breast tissue. *Appl. Opt.* 37:798. DOI: https://doi.org/10.1364/ao.37.000798.

Moulton K. et al. (2006) Use of glycerol as an optical clearing agent for enhancing photonic transference and detection of Salmonella typhimurium through porcine skin. *J. Biomed. Opt.* 11 (5): 054027. DOI: https://doi.org/10.1117/1.2363366.

Niemz M. H. (2014) *Biological and medical physics, biomedical engineering: Laser-tissue interactions,* no. 1

Oliveira L. M. C., Tuchin V. V. (2019) *The Optical Clearing Method,* DOI: https://doi.org/10.1007/978-3-030-33055-2.

Parsa P., Jacques S. L., Nishioka N. S. (1989) Optical properties of rat liver between 350 and 2200 nm. *Appl. Opt.* 28 (12): 2325. DOI: https://doi.org/10.1364/ao.28.002325.

Samatham R., Phillips K. G., Jacques S. L. (2010) Assessment of optical clearing agents using reflectance-mode confocal scanning laser microscopy. *J. Innov. Opt. Health Sci.* 3 (3): 183–188. DOI: https://doi.org/10.1142/S1793545810001064.

Sardar D. K., Mayo M. L., Glickman R. D. (2001) Optical characterization of melanin. *J. Biomed. Opt.* 6 (4): 404. DOI: https://doi.org/10.1117/1.1411978.

Shanshool A. S., Ziaee S., Ansari M. A., Tuchin V. V. (2024) Advances in the transport of laser radiation to the brain with optical clearing: From simulation to reality. *Prog. Quantum Electron* 94:100506. DOI: https://doi.org/10.1016/j.pquantelec.2024.100506.

Shariati B., Ansari M. A., Khatami S. S., Tuchin V. V. (2023) Multimodal optical clearing to minimize light attenuation in biological tissues. *Sci. Rep.* 13 (1): 21509. DOI: https://doi.org/10.1038/s41598-023-48876-x.

Shariati B., Khatami S. S., Ansari M. A., Jahangiri F., Latifi H., Tuchin V. V. (2022) Method for tissue clearing: temporal tissue optical clearing. *Biomed. Opt. Express* 13 (8): 4222. DOI: https://doi.org/10.1364/boe.461115.

Sudheendran N., Mohamed M., Ghosn M. G., Tuchin V. V., Larin K. V. (2010) Assessment of tissue optical clearing as a function of glucose concentration using optical coherence tomography. *J. Innov. Opt. Health Sci.* 03 (03): 169–176. DOI: https://doi.org/10.1142/S1793545810001039.

Tuchin V. V. (2015) *Tissue optics: Light scattering methods and instruments for medical diagnosis: Third edition* Society of Photo-Optical Instrumentation Engineers (SPIE) DOI: https://doi.org/10.1117/3.1003040.

Tuchin V. V., Xu X., Wang R. K. (2002) Dynamic optical coherence tomography in studies of optical clearing, sedimentation, and aggregation of immersed blood. *Appl. Opt.* 41 (1): 258. DOI: https://doi.org/10.1364/ao.41.000258.

Tuchin V. V., Zhu D., Genina E. A. (2021) *Handbook of Tissue Optical Clearing.* Boca Raton: CRC Press DOI: https://doi.org/10.1201/9781003025252.

Tuchina D. K., Genin V. D., Bashkatov A. N., Genina E. A., Tuchin V. V. (2016) Optical clearing of skin tissue ex vivo with polyethylene glycol. *Opt. Spectrosc. (English Transl. Opt. i Spektrosk.)* 120 (1): 28–37. DOI: https://doi.org/10.1134/S0030400X16010215.

Tuchina D. K., Timoshina P. A., Tuchin V. V., Bashkatov A. N., Genina E. A. (2019) Kinetics of Rat Skin Optical Clearing at Topical Application of 40%Glucose: *Ex Vivo* and *in Vivo* Studies,. *IEEE J. Sel. Top. Quantum Electron.* 25 (1) DOI: https://doi.org/10.1109/JSTQE.2018.2830500.

Wang J., Ma N., Shi R., Zhang Y., Yu T., Zhu D. (2014) Sugar-Induced Skin Optical Clearing: From Molecular Dynamics Simulation to Experimental Demonstration. *IEEE J. Sel. Top. Quantum Electron.* 20 (2): 256–262. DOI: https://doi.org/10.1109/JSTQE.2013.2289966.

Wang L., Jacques S. L., Zheng L. (1995) MCML-Monte Carlo modeling of light transport in multi-layered tissues. *Comput. Methods Programs Biomed.* 47 (2): 131–146. DOI: https://doi.org/10.1016/0169-2607(95)01640-F.

Wilson B. C., Adam G. (1983) A Monte Carlo model for the absorption and flux distributions of light in tissue. *Med. Phys.* 10 (6): 824–830. DOI: https://doi.org/10.1118/1.595361.

Yaroslavsky A. N., Schulze P. C., Yaroslavsky I. V., Schober R., Ulrich F., Schwarzmaier H. J. (2002) Optical properties of selected native and coagulated human brain tissues in vitro in the visible and near infrared spectral range. *Phys. Med. Biol.* 47 (12): 2059–2073. DOI: https://doi.org/10.1088/0031-9155/47/12/305.

Zhu D., Larin K. V., Luo Q., Tuchin V. V. (2013) Recent progress in tissue optical clearing. *Laser Photonics Rev.* 7 (5): 732–757. DOI: https://doi.org/10.1002/lpor.201200056.

Ziaee S., Ansari M. A., Maleki V. Ghotbi, Ebrahimi S. Nejad (2023) Investigating the effect of using semi-natural polymer HPMC in optical clearing of mice skin. *J. Lasers Med.* 20 (2): 5–12. https://icml.ir/article-1-618-en.html

Zonios G., Dimou A. (2009) Light scattering spectroscopy of human skin *in vivo*. *Opt. Express* 17 (3): 1256. DOI: https://doi.org/10.1364/oe.17.001256.